9.2 NUMERICAL ANALYSIS OF MAP IOP 15 CYCLOGENESIS AND ASSOCIATED PRECIPITATION

Andrea Buzzi*, Massimo D'Isidoro, and Silvio Davolio
ISAC-CNR, Bologna, Italy

1 INTRODUCTION

The first period (namely 6-7 Nov. 1999) of MAP IOP 15 was characterised by the rapid development of an orographic cyclone south of the Alps and the passage of an intense cold front, coming from northwest, over the massif. Energetic mesoscale phenomena were associated with the weather evolution: strong and damaging winds, modulated or caused by the orography, heavy precipitation, at least partly of orographic nature, both south of the Alps, in the so called "Lago Maggiore MAP target area" (Bougeault et al., 2001) and over the Friuli-Veneto area, and then more to the south, over the northern Apennines, in the strong post-frontal north-easterly flow. In a previous work (Buzzi and Davolio, 2001) the impact of the different orography representations on the cyclone development was investigated and an enhancement of the topography showed beneficial effects on the forecasted geopotential field. In the present work, employing such a modified orography representation, a reanalysis of the initial condition is applied in order to obtain a further reduction of the forecast error and a better description of the mesoscale phenomena. The MAP SOP observing facilities provide an almost unique opportunity to study this event in detail and to assess the model performance.

2 THE OBJECTIVE REANALYSIS AND THE NUMERICAL EXPERIMENTS

The model used in this study is BOLAM (Buzzi and Foschini, 2000), version 2001, which employs the advanced ECMWF radiation scheme (Morcrette et al., 1998). Two different resolutions are adopted in this study, by implementing a nesting strategy. In the low resolution experiments, a grid of 160×160 points was used, with a grid spacing of 0.2 deg (rotated coordinates) and 38 vertical levels. In the nested experiments, the horizontal resolution is 0.06 deg (260×260 grid points) with 44 vertical levels. In order to obtain a reanalysis of the initial condition for the case study, an objective analysis, based essentially on the

**Corresponding author address:* Andrea Buzzi, ISAC-CNR, via Gobetti 101, Bologna 40129, Italy; email: A.Buzzi@isac.cnr.it

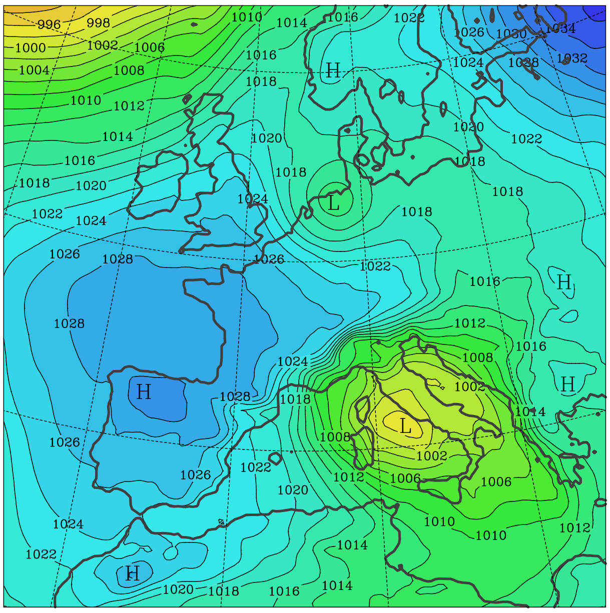

Figure 1: MSLP after 30 h of low resolution simulation, verifying 07 Nov. 1999, 06 UTC.

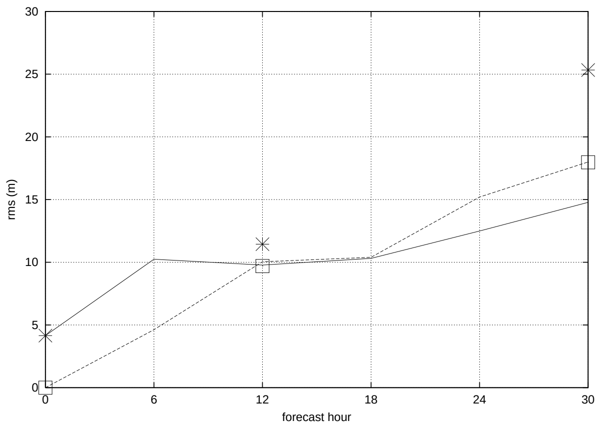

Figure 2: RMSE for geopotential height at 500 hPa. The two curves represent the RMSE of the simulations starting from ECMWF analysis (dashed line) and from reanalysis (solid line) calculated with respect to the ECMWF analyses. The symbols are the RMSE calculated versus reanalyses for the simulation starting from ECMWF analysis (stars) and from reanalysis (squares).

Optimum Interpolation technique algorithm tuned for mesoscale, is applied to the ECMWF (background) fields, re-assimilating standard and assimilating additional GTS-type data to define model initial condition and verification fields. In addition to the Optimal Interpolation algorithm, an initialisation has been adopted in order to reduce unbalances.

Fig. 1 shows the total field of the low resolution reanalysis experiment after 30 hours of integration. At this verification time (07 Nov., 06 UTC) the lee cyclone is fully developed with its centre located over the Tyrrhenian Sea, while the "parent" cyclone is identified over Denmark. The two cyclones are well separated by a strong pressure ridge north of the Alps. The general improvement in the forecast using the reanalysis as initial condition can be appreciated by computing RMS errors over the model domain. Fig. 2 shows the RMSE computed for the geopotential height at 500 hPa relative to 30 hour forecasts starting at 00 UTC, 6 November. The two curves represent the RMSE with respect to the ECMWF analyses calculated every 6 hours, for the twin forecasts starting from the ECMWF analysis and from the reanalysis, respectively. The figure shows a reduction of RMSE in the reanalysis run after 30 hours of about 3 m. A similar result holds for the geopotential height at levels below and above. Note that the error growth is smaller for the run starting with the reanalysis. The improvement in term of RMSE of the forecast starting from the reanalysis field is still more evident if it is calculated against the reanalyses themselves rather than the ECMWF analyses (compare symbols in fig. 2). In this case, after 30 hours, the RMSE is about 8 m lower than for the control forecast.

3 MESOSCALE ASPECTS

The mesoscale patterns of the case study have been analysed in the high resolution experiments, nested in the lower resolution run, starting at 06 UTC of 06 November, after 6 hours of integration over the coarse domain. Two experiments have been performed, one from the coarse integration starting from the unmodified ECMWF analysis (exp. SN: "son, no reanalysis"), the other from the coarse integration starting from the reanalysed field (exp. SR: "son, reanalysis").

The evolution of the wind field at 850 hPa, representative of the flow impinging on the Alps, is shown in Fig. 3 (exp. SR). At 12 UTC the cold front extends from Germany to the western Alps and the Pyrenees, with a protrusion already affecting the Gulf of Lyon. A southerly to southeasterly prefrontal flow (Fig. 3a) produces at this time moderate rain in the Lago Maggiore area, intensifying in the subsequent hours (see the composite radar images, available at the MAP Data Centre: "http://www.map.ethz.ch/sop-doc/panel/visrad_master.html"). Fig. 3b shows that by 18 UTC the flow has become northerly all over the Piedmont region and the Ligurian sea, taking the shape of a low level jet, while a mesoscale vortex is now clearly developed over the central Po valley, with southeasterly flow rising above the colder northerly flow in the area around Milano, contributing to the moderate-to-heavy rain in this area observed in the period between 15 and 21 UTC (accumulation up to about 50 mm). At this time the equivalent potential temperature θ_e at the same level (not shown) shows clearly a tongue

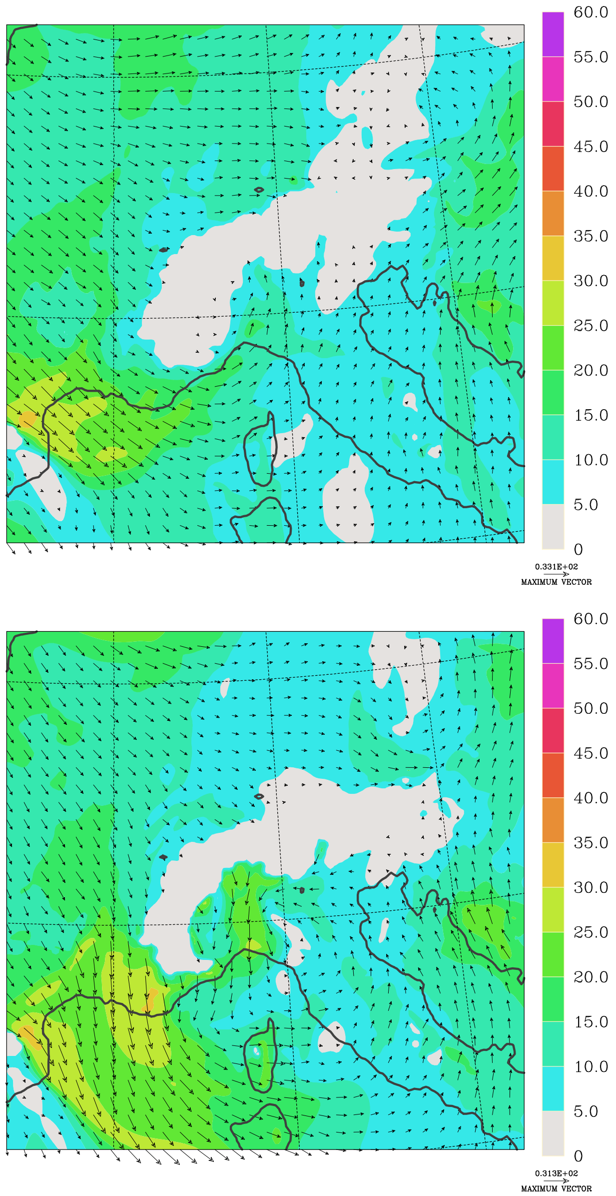

Figure 3: Wind at 850 hPa after 6 hours of high resolution simulation (top), verifying 06 Nov. 1999, 12 UTC; after 12 hours of simulation (bottom), verifying 06 Nov. 1999, 18 UTC.

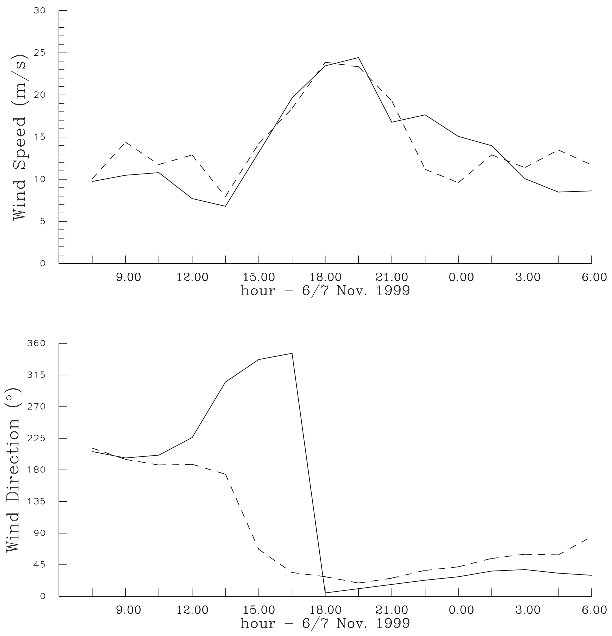

Figure 4: Wind speed (top panel) and wind direction (bottom panel) measured by the wind profiler located at Lonate Pozzolo (dashed line) at 2640 m a.s.l. and forecasted by the model in the same location at 750 hPa (solid line).

of low θ_e values in the area of northerly flow south of the Alps, bounded by higher values. This tongue of low θ_e does not correspond to a clear minimum in temperature at the level of 850 hPa, indicating that the air is dry and warmed by the descent past the Alps. The rapid evolution of the wind field south of the Alps is clearly documented by the French wind profiler that was located in Lonate Pozzolo (45.57 N, 8.72 E) (Fig. 4). Between 13.30 and 15 UTC the wind direction at 2640m suddenly rotates and by 18 UTC the wind speed reaches the maximum value of about 25 m/s. For the same location and approximately the same height the model is in quite good agreement with the data as far as the wind speed is concerned (Fig. 4a), but there is an evident difference in the rotation of the wind (fig. 4b). While the model shows a veering, the radar reveals a backing of the wind that by 15 UTC becomes northerly. This is probably due to a slight meridional displacement of the centre of cyclonic rotation of the mesoscale vortex. The reanalysis experiment shows a slight improvement, with respect to the control one, in the onset of the wind rotation (not shown).

4 PRECIPITATION

The analysed episode is characterised by three phases of rainfall. At the beginning of the period, associated with the southwesterly flow, a first stage of light orographic precipitation is observed over the Lago Maggiore target area. As the flow becomes northerly and the vortex develops in the Po valley, a second phase of intense precipitation around Milano takes place. Starting approximately at the same time, a period of mainly convective rain associated with scattered thunderstorms (as revealed by the lightening networks) affects an area from the northern Adriatic to the southern slope of the Alps in the Veneto-Friuli area. Then the strong and persistent northeasterly flow produces heavy orographic precipitation over the northern Apennines during the first half of 7 November. The 24 hours accumulated precipitation (starting from 06 Nov., 06 UTC) for the two experi-

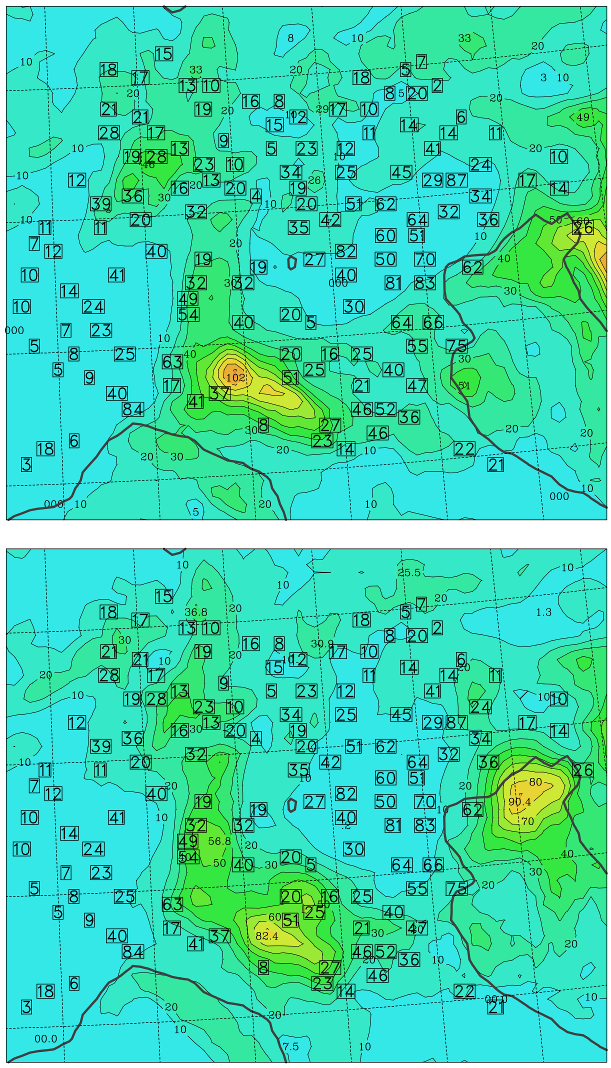

Figure 5: 24 hours accumulated precipitation from 06 Nov. 1999, 06 UTC for experiment SN (top panel) and SR (bottom panel). Selected observational values of rainfall are plotted.

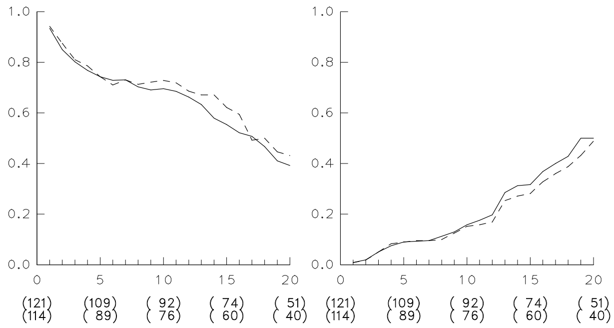

Figure 6: Hit rate score (left) and False alarm score (right) for experiment SN (solid line) and SR (dashed line). Rainfall thresholds on x-axis are in mm/24h. Numbers in brackets indicate number of observations (upper) and model grid points (lower) exceeding the threshold.

ments (SN and SR) is shown in fig. 5, together with selected rain gauge observations of the MAP dataset. The rainfall field of the SR forecast is clearly improved around the area of Milano, where the precipitation is still slightly displaced eastward, but the intensity is closer to the reality.

Both model experiments, however, are affected by a large precipitation error over the central-eastern Prealpine region where convective activity coming from the Adriatic Sea produced locally large amounts of rain late in the afternoon of 06 November. The model seems to anticipate the frontal passage over this part of the Alps. Anyway, precipitation scores calculated for the north-west Alpine area and for the Apennines indicate a slight improvement of the SR over the SN experiment (fig. 6). Considering the whole domain, no improvement is revealed by the scores (not shown), due mainly to the persistence of the precipitation forecast error in the central-eastern Alpine sector.

5 CONCLUSIONS

The MAP IOP 15 was characterised by a strong event of Alpine lee cyclogenesis, associated with rapidly changing meteorological phenomena in the region south of the Alps. The formation of a small scale vortex, the onset of strong winds following the cold front, the evolution of the precipitation field, partly associated with orographic rain, have been described in short, also by comparing observations with mesoscale model results. However, the model simulations of this event are characterised by a relatively large scale error structure which is partly associated with the representation of the orographic forcing and partly with the initial conditions (besides possible model errors). In fact, a simple enhancement of the orography and a reanalysis of the initial condition, the latter to be intended mainly as a refinement of mesoscale structures associated with the resolution adopted (20 km for the analysis grid), contribute to reduce model errors, more evident in the geopotential and upper PV fields. In particular, they concur to a more pronounced and rapid, although still not totally correct, cut off process.

The finer scale nested experiments, devoted to describe the mesoscale structures, reveal some sensitivity to the differences in the initial conditions of the parent runs, therefore maintaining the forecast improvements introduced by the reanalysis. Such improvements, though not large, characterise also the precipitation fields over north-western Italy, preceding and accompanying the propagation of the cold front and of the lee vortex. However, a large deficit of model precipitation along the southern slope of the eastern Alps seems to resist both reanalysis and changes in orographic representation. For this reason, further attention will be put on the analysis of humidity, including application of rainfall assimilation techniques, in order to better understand the origin of model errors and to reveal possible relationships between the precipitation and the cut off evolution.

Acknowledgements

This work has been supported by the CNR-GNDCI project "Remote sensors and extreme precipitations" and by the ASI/ARS/99-62 ASTRO project.

References

Bougeault, P., P. Binder, A. Buzzi, R. Dirks, R. Houze, J. Kuettner, R.B. Smith, R. Steinacker, H. Volkert, 2001: The MAP special observing period. *Bull. Amer. Met. Soc.*, **82 (3)**, 433–462.

Buzzi, A., and S. Davolio, 2001: Effects of orographic representation on simulations of cyclone development and mesoscale aspects of IOP 15. *MAP Newsletter*, **15**, 80–83.

Buzzi, A., and L. Foschini, 2000: Mesoscale meteorological features associated with heavy precipitation in the southern Alpine region. *Meteorol. Atmos. Phys.*, **72**, 131–146.

Morcrette, J. J., S. A. Clough, E. J. Mlawer, and M. J. Iacono, 1998: Impact of a validated radiative transfer scheme, RRTM, on the ECMWF model climate and 10-day forecasts. *ECMWF Technical Memo.*, **252**, 47 pp.